Supporting Information

Unprecedented Neptunyl(V) Cation-Directed Structural Variation in Np_2O_x compounds

Zhong-Fei Xu#,[a,b] Wen-Jing Zhang#,[a,b] Ping Zhang,[c] Shu-Xian Hu,*[a,b]

[a] Department of Physics, University of Science and Technology Beijing, Beijing 100083, China.

[b] Beijing Computational Science Research Center, Beijing, 100193, China. [c] Institute of Applied Physics and Computational Mathematics, Beijing, 100088, China

*Corresponding Authors: hushuxian@csrc.ac.cn (S.X.H)

Computational details:

First, the stable crystal structures of Np_2O_x with different stoichiometric ratios were predicted using particle-swarm optimization methodology based Crystal Structure Analysis by Particle Swarm Optimization (CALYPSO) code.[1] Electronic structures of Np_2O_x were performed using density functional theory within the Perdew-Burke-Ernzerhof parameterization of the generalized gradient approximation (GGA),[2] as implemented in the Vienna Ab initio Simulation Package (VASP) code.[3-6] The lattice constants are a = b = c =15 Å. Spin-polarized local density approximation calculations with the Hubbard potential[7] were carried out for Hubbard correction; meanwhile, an U_{eff} value of 4 V was used to Np 5f electrons in all calculations. The projector augmented wave (PAW) method[6] was employed to describe electron–ion interactions. Brillouin zone (BZ) sampling is used by Gamma only k-point. The plane-wave basis cut-off set as 500 eV. Equilibrium geometries were obtained by the minimum energy principle until the energy and force is converged to 10^{-5} eV and 0.02 eV/Å, respectively.

Then, the generalized gradient approximation (GGA) with the PBE functional[8] implemented in the Amsterdam Density Functional program ADF 2016.107 was used to optimize the geometries.[9] The Slater type orbital (STOs) of the quality of triple-ξ plus two polarization functions (TZ2P)[10] with a frozen [$1s^2$–$5d^{10}$] shell for Np atom and a frozen [$1s^2$] shell for O were used. The relativistic effects were accounted for by using the scalar relativistic (SR) and spin-orbit (SO) zero-order-regular approximation (ZORA).[11] Further, the domain based local pair-natural orbital based singles and doubles coupled cluster method (DLPNO-CCSD(T))[12] implemented with *ab initio* wave-function theory (WFT) calculations being carried out in the ORCA program[13] along with the segmented all-electron relativistic contracted basis sets with DKH2-Hamiltonians (SARC-DKHTZVP) for Np and DKH-def2-TZVPP for O was used to run single-point calculations for checking the relative energies of each Np_2O_x species.[14]

Bond order analyses based on the Mayer method (BO_{Mayer}),[15] the Gopinathan–Jug method ($BO_{G–J}$)[16] and Nalewajski−Mrozek method (BO_{NM})[17] were performed to evaluate the bond strength. The population partitioning schemes of Mulliken were used to determine the atomic charges of atoms in these species.

Multiconfigurational complete active space (CASSCF) calculations followed by second-order perturbation theory (CASPT2)[18] were performed at the DFT optimized geometries of Np_2O_3. Scalar relativistic effects were included by use of the Douglas-Kroll-Hess Hamiltonian[19, 20] and the relativistic all electron ANO-RCC basis sets with double-ζ quality (ANORCC-VDZP)[21] with the following contractions: [8s7p5d3f1g] for neptunium and [3s2p1d] for oxygen. The CASSCF/CASPT2 calculations[22] were performed with the OpenMOLCAS package.[23] The Cholesky decomposition technique in all CASSCF/CASPT2 calculations combined with the local exchange screening was employed to reduce the computational costs for the two-electron integrals. The CASSCF/CASPT2 approach is successful in studying many actinide-containing systems. The active spaces for the ground state and the lowest excited states of Np_2O_3 contained the highest four occupied orbitals of O_b 2p character (cf. Figure S3), i.e., $1a'_2$, $7e'{:}_1$, $7e'{:}_2$, $6a''_2$, and eight Np-5f based unpaired orbitals and four virtual orbitals dominated by Np-6d character. This selection of active space gives 16 orbitals with 16 electrons, denoted as CAS(16e, 16o). State-averaged CASSCF calculations[22] based on this selection of active space were carried out to generate the wavefunctions for the ground and singlet- and triplet- excited states corresponding to single-electron transition from O-2p orbitals to Np-5f orbitals in Np_2O_3.

Results

Np_2O. Because neptunium has an $5f^4 6d^1 7s^2$ ground electron configuration and the electron spin multiplicities of the Np_2O clusters are determined by the orientation of the metal-based electrons, we considered two spin states, 11 and 13. The lowest energy state (**1A** in Table S1) found for Np_2O is a $^{11}A_2$ state with the 10 valent electrons in Np 5f based molecular orbitals (MOs) and two valent electrons in Np 7s based MOs, consisting of an electronic configuration of $(f_{Np1})^5(f_{Np2})^5(s_{Np1})^1(s_{Np2})^1$. Note that we refer to the $12a_1$ orbital that is the in-phase combination of the 7s orbitals on the two Np centers as σ_{ss}, and the associated out-of-phase $16a_1$ orbital as σ_{ss}*, because it allows direct comparison with nearly identical MO's of the other species. The electronic structure for $^{13}B_2$ state (**1B**) of Np_2O that having 12 unpaired electrons in the 5f subshell is of more to be 0.674 eV (PBE+U) or 0.568 eV (DLPNOCCSD(T)) higher in energy than the ground state. The $^{11}A_2$ state Np_2O structure have two Np-O_b bonds with the same length of 2.063 Å, where O_b denotes the bridging oxygen atom, and a Np-O_b-Np bond angle of 105.7 deg., which could be considered as extended from 96.1 deg. in the $^{13}B_2$ state where a one-electron-two-center (1e-2c) $\sigma_{\phi\phi}$ bond was formed between two Np atoms. This transformation of bond angle shows that the $\sigma_{\phi\phi}$ bond is unfavorable largely due to the its localized orbital radials arising the sharply strong Pauli repulsion.

Np_2O_2. Results of calculations on Np_2O_2 (Table S2) are consistent with the $(f_{Np1})^4(f_{Np2})^5(s_{Np1})^1$ electronic configuration, with a predicted $^{11}B_{1g}$ ground state (**2A**). This lowest energy structure has a D_{2h} symmetry, which is 2.608 eV lower than the second isomer (**2B**) where Np_2O_2 has a C_1 symmetry Np-O-Np-O structure. In D_{2h} Np_2O_2, the Np-O bond length is 2.086 Å, the Np-Np bond length is 3.260 Å and the O-O bond length is 2.603 Å.

Np_2O_3. The ground state Np_2O_3 can be described as a $^9E''$ state (**3A** in Table S3), having $(f_{Np1})^4(f_{Np2})^4$ valence orbital occupancy with the two Np atoms having oxidation states of +III. The mixture valent Np(II)/Np(IV) ^9A state (**3B**) consisting of an electronic configuration of $(f_{Np1})^5(f_{Np2})^3$ is predicted to be 1.089 eV higher in energy than **3A**. The **3A** has a D_{3h} symmetry structure with three Np-O bonds of the same bond length of 2.105 Å. Unexpectedly, the Np-Np bond reduce to 2.943 Å from the 3.260 Å in Np_2O_2 and even shorter than the 3.087 Å in the unfavorable **1B** where the f-f interaction is observed, which could be resulted from the constrained D_{3h} structure and the strong f-f bonding in **3A**. As the electronic structures of SOMOs for $^9E''$ Np_2O_3 shown in Figure S3, the MO 8a'$_1$ is an obvious f-f bond, composed of coaxial orbital interactions between two f_{z3} AOs (Listed in Table S4). Thus, the bond order of this Np-Np bond is 0.55 by Mayer method (Table S9).

Np_2O_4. Four isomers (Table S5) have been found from the global minimum searching and the C_s symmetry one (**4A**) has been predicted to be the lowest-energy one. It consists of one Np(V) and one Np(III) with the total valent electronic structure of $(5f_{Np1})^2(5f_{Np2})^4$. As evident by the wave-function graphics in Figure 3, the lowest two SOMOs, 15a" and 29a' have major Np1 5f characters and the other four SOMOs, 32a', 16a", 31a' and 30a' are located in Np2. This rank also proves that Np1 has higher oxidation state than the Np2, because the higher oxidation state Np has the stronger spin-polarization effects and thus its valence energy levels are in lower energy range. The other three energetic competitors (**4B**, **4C** and **4D**) share the same the orbital occupancy of $(5f_{Np1})^3(5f_{Np2})^3$ with two Np(IV) atoms, which were calculated to be more than 0.700 eV higher in energy than the **4A**. These three isomers contain two quasi-tetrahedral NpO_3, and the two terminal oxygen (O_t) ions are placed on the opposite sides of the Np_2O_2 plane of the tetrahedron (see Table S11 for the coordinates). This phenomenon can be manifested through the near-degenerated 5f energy levels in low-valent Np ions that significantly complicates the structures of Np_2O_4. Interestingly, transferring one electron from Np1 5f-based MO to O 2p shell results in a mixture valent state of Np(V) and Np(III) and greatly stabilizes the structure of Np_2O_4. The lowest-energy **4A** featuring mixed Np(III)/Np(V) has two coordination types for Np. The Np(III) has a quasi-tetrahedral type with the three Np-O single bonds of *ca.* 2.000 Å, while the Np(V) exists in a $[O_t{=}Np(V){=}O_b]^+$ fragment where the Np(V) presents a octahedral coordination type, *e.g.* the O=Np bond lengths of 1.811 Å and 1.972 Å, and the bond angle O_t1-Np1-O_b3 of 178.3 deg. as well as the bond angle O_t1-Np1-O_b1/O_b2 of 105.4 deg., as known as a Np(V) structural feature. In this bonding feature, two Np atoms are in a very close distance of 2.994 Å, which is of unprecedented structure and oxidation state of Np. And with the formation of Np(V), the bond angle transfers from bent to linear, which is largely ascribed to the 5f-participant in the chemical bonding of Np-O. Such as the Np=O_t bonding MO 28a' in **4A** was composed by 24.85% of Np1 5f orbital into the bonding, 6.05% larger in contribution comparing to 18.80% of Np1 5f in $20a_g$ MO in **4C**. This phenomenon has been found as the unique feature for f-orbitals that the participation of f orbitals in chemical bonding could direct the structure of a compound. [24, 25]

Np_2O_5. Global minimum searching combined with full geometry optimization performed at DFT level resulted in only two structures corresponding to potential energy minima shown in Table S6. Both structures have C_2 symmetry. The energetically preferred structure (**5A**) consists of one rhombic Np_2O_4 where two neptunyl cations show a typical T-shape cation-cation interaction (CCI).[add refs] and a bridging oxygen atom (O_b), while the second isomer (**5B**) consisting of a two-parallel-NpO_2 units bonded by an O_b is calculated to be 0.63 eV higher in energy than the **5A**. The **5A** has a $(5f_{Np1})^2$-$(5f_{Np2})^2$ valence configuration and Np has an oxidation state of +V, which could be considered as the fifth oxygen atom consequently oxidizing the Np2(IV) atom in Np_2O_4 into a Np(V). This mechanism is evocative of how the stabilization of the Np(V). In the structure of **5A**, the Np-O_t bond lengths in neptunyl are 1.802 Å and 1.899 Å, while the Np-O_b bond length is 2.103 Å. As shown in Figure 5, the Np_2O_5 has four singly occupied MOs being 5f characters: two $5f_\delta$ and two $5f_\phi$, and has ten-unoccupied 5f-based MOs and finally settles on two Np(V) metals.

Np_2O_6. We found that the lowest energy isomer of Np_2O_6 is a D_{2h} structure (**6A** in Table S7). The **6A** is a triplet $^3B_{2u}$ state with the electronic structure of $5f^1$-$5f^1$ on Np atoms, thus each Np has a hexavalent oxidation state. The most competing local minimum (**6B**) where a NpO_2 vertically is bonded to a planar NpO_4 structure, is 2.425 eV higher in energy above the **6A**. Interestingly, this isomer exhibits a mixed valent as the electronic configuration being $(5f_{Np1})^2$-$(5f_{Np2})^0$. The **6C**, the isometric to **6B** in different orientation of the NpO_2 and NpO_4 was aroused from the settled-up spin state, being 1.117 eV less stable than **6A**. The fourth isomer (**6D**) with a valent electronic structure of $(5f^2)$-$(5f^2)$ and two pentavalent Np atoms is 2.409 eV less stable, where two penta-valent neptunyl cations were bridged by a peroxide anion in the structure. It is worth mentioning that the oxidation states of di-Np(VII) in **6A** is obviously stable than the mixture valent Np(V)/Np(VII) in **6B** and **6C** or the di-Np(V) in **6D**. In other words, Np favors Np(VI) for Np_2O_6. This global minimum D_{2h} structure is made up of two linear $Np(V)O_2$ with the Np-O_t bond lengths of 1.792 Å and the two bridging oxygen atoms (O_b) that binds two Np atoms within the Np-O_b-Np-O_b plane at 2.100 Å from the point of the Np and O_b. The electronic structures of the SOMOs of Np_2O_6 are shown in Figure S6. There are two single electrons are kept on Np: one $5f_\delta$- and one $5f_\phi$- based MOs, $8b_{2u}$ and $12a_g$. There are 12 unoccupied 5f-bases MOs, except the $5f_\sigma$ orbitals, spanning within a narrow band (1.648 eV). And the LUMO-SOMO gap is only 0.096 eV, suggesting that it manifests itself in the makeup of valence 5f orbitals rather than energy. The lowest-excitations would occur to 5f to 5f transitions.

Np_2O_7. The Np_2O_7 has been found as a representative to show robustly energetic stability of the high-oxidation state structure. Table S8 shows optimized low-lying energy structures found by the structure search, with their symmetry and energy relative to the ground-state C_s structure (**7A**), and their Cartesian coordinates are given in Tables S11. The lowest stable isomer is a closed-shell singlet 1A' with the electronic structure of $5f^0$ on Np, thus a compound featuring heptavalent Np has been predicted. The lowest metastable isomer **7B**, which structurally identical with the 1Cs but in a triplet spin state, is less stable than the ^1C_s by 0.055 eV in energy, consisting of $(2p_O)^1(5f)^1$ electronic configuration. There emerges another metastable state ^3A with a $(5f)^1(5f)^1$ electronic structure (isomer **7C**), but 0.460 eV higher in energy than the ^{1}Cs. For the isomer **7D**, isomeric to the **7C** being slightly higher energy than **7C**, the closed-shell ^1A consisting of a spin-up $(5f_\delta)^1$ and a spin-down $(5f_\pi)^1$ due to the broken-symmetry calculation, thus showing that Np still retains its VI oxidation state in isomer **7D**. In the ground $^1A'$ state, the Np1 is bounded by two terminal oxygen atoms with the Np1-O_t bond length of 1.787 Å, by one actinyl oxygen with the Np1-O_t bond length of 1.961 Å and by one bridging oxygen with the Np1-O_b bond length of 2.013 Å, while the Np2 is bounded by three terminal oxygen atoms with the Np2-O_t bond length of 1.797, 1.797, 1.846 Å and by one bridging oxygen with the Np1-O_b bond length of 2.236 Å. Although the structure looks strange, each Np has effective four coordinated oxygen atoms, consisting of two Np-O single bonds and three Np=O double bonds. This structure could be understood as two quasi-planar NpO_3^+ cations connected by a O^{2-} anion. The electronic structures of the HOMOs and LUMOs of Np_2O_7 is shown in **Figure S7**. The lowest 14 unoccupied MOs are mainly localized on Np 5f orbitals and the top of occupied MOs are bonding orbitals with an adiabatic polarization of the O 2p orbitals toward the Np 5f shell, and thus Np has an oxidation state of VII. And the bonding between Np and the oxide mainly occurs between the 5f orbitals of Np and 2p of O^{2-} and there is also some of 6d orbitals mixed into the bonding. suggesting that 5f orbitals participate in the chemical bonding in the high Np compounds. Taking the Np2-O bonding orbital 19a" as an example, there are mainly composed of 36.8% of the 5f orbitals and 58.3% of the 2p orbitals into the bonding.

References

1. Wang, Y.; Lv, J.; Zhu, L.; Ma, Y., CALYPSO: A method for crystal structure prediction. *Computer Physics Communications* **2012,** *183* (10), 2063-2070.
2. Perdew, J. P.; Burke, K.; Wang, Y., Generalized gradient approximation for the exchange-correlation hole of a many-electron system. *Physical Review B* **1996,** *54* (23), 16533.
3. Kresse, G.; Hafner, J., Ab initio molecular dynamics for liquid metals. *Physical Review B* **1993,** *47* (1), 558.
4. Kresse, G.; Furthmüller, J., Efficiency of ab-initio total energy calculations for metals and semiconductors using a plane-wave basis set. *Computational materials science* **1996,** *6* (1), 15-50.

5. Käckell, P.; Furthmüller, J.; Bechstedt, F.; Kresse, G.; Hafner, J., Characterization of carbon-carbon bonds on the SiC(001)c(2× 2) surface. *Physical Review B* **1996,** *54* (15), 10304.

6. Kresse, G.; Joubert, D., From ultrasoft pseudopotentials to the projector augmented-wave method. *Physical Review B* **1999,** *59* (3), 1758.

7. Dong, C.; Persson, C.; Vayssieres, L.; Augustsson, A.; Schmitt, T.; Mattesini, M.; Ahuja, R.; Chang, C.; Guo, J.-H., Electronic structure of nanostructured ZnO from x-ray absorption and emission spectroscopy and the local density approximation. *Physical Review B* **2004,** *70* (19), 195325.

8. Perdew, J. P.; Burke, K.; Ernzerhof, M., Generalized gradient approximation made simple. *Physical review letters* **1996,** *77* (18), 3865.

9. Averill, F. W.; Ellis, D. E., An efficient numerical multicenter basis set for molecular orbital calculations: application to FeCl4. *The journal of chemical physics* **1973,** *59* (12), 6412-6418.

10. Van Lenthe, E.; Baerends, E. J., Optimized Slater-type basis sets for the elements 1–118. *Journal of computational chemistry* **2003,** *24* (9), 1142-1156.

11. Lenthe, E. v.; Baerends, E.-J.; Snijders, J. G., Relativistic regular two-component Hamiltonians. *The Journal of chemical physics* **1993,** *99* (6), 4597-4610.

12. Guo, Y.; Riplinger, C.; Liakos, D. G.; Becker, U.; Saitow, M.; Neese, F., Linear scaling perturbative triples correction approximations for open-shell domain-based local pair natural orbital coupled cluster singles and doubles theory [DLPNO-CCSD(T0/T)]. *The Journal of chemical physics* **2020,** *152* (2), 024116.

13. Neese, F., The ORCA program system. *Wiley Interdisciplinary Reviews: Computational Molecular Science* **2012,** *2* (1), 73-78.

14. Pantazis, D. A.; Neese, F., All-electron scalar relativistic basis sets for the lanthanides. *Journal of chemical theory and computation* **2009,** *5* (9), 2229-2238.

15. Mayer, I., J. Quantum Chem. 1986, 29, 73. Mayer, I. J. *Quantum Chemistry* **1986,** *29*, 477.

16. Gopinathan, M.; Jug, K., Valency. I. A quantum chemical definition and properties. *Theoretica chimica acta* **1983,** *63* (6), 497-509.

17. Michalak, A.; DeKock, R. L.; Ziegler, T., Bond multiplicity in transition-metal complexes: applications of two-electron valence indices. *The Journal of Physical Chemistry A* **2008,** *112* (31), 7256-7263.

18. Celani, P.; Werner, H.-J., Multireference perturbation theory for large restricted and selected active space reference wave functions. *The Journal of Chemical Physics* **2000,** *112* (13), 5546-5557.

19. Douglas, M.; Kroll, N. M., Quantum electrodynamical corrections to the fine structure of helium. *Annals of Physics* **1974,** *82* (1), 89-155.

20. Hess, B. A., Relativistic electronic-structure calculations employing a two-component no-pair formalism with external-field projection operators. *Physical Review A* **1986,** *33* (6), 3742.

21. Pierloot, K.; Dumez, B.; Widmark, P.-O.; Roos, B. O., Density matrix averaged atomic natural orbital (ANO) basis sets for correlated molecular wave functions. *Theoretica chimica acta* **1995,** *90* (2), 87-114.

22. Schmidt, M. W.; Gordon, M. S., The construction and interpretation of MCSCF wavefunctions. *Annual review of physical chemistry* **1998,** *49* (1), 233-266.

23. Aquilante, F.; Autschbach, J.; Carlson, R. K.; Chibotaru, L. F.; Delcey, M. G.; De Vico, L.; Fdez. Galván, I.; Ferré, N.; Frutos, L. M.; Gagliardi, L., Molcas 8: New capabilities for multiconfigurational quantum chemical calculations across the periodic table. Wiley Online Library: 2016.

24. Zhang, W.-J.; Wang, G.-J.; Zhang, P.; Zou, W.; Hu, S.-X., The decisive role of 4f-covalency in the structural direction and oxidation state of XPrO compounds (X: group 13 to 17 elements). *Physical Chemistry Chemical Physics* **2020,** *22* (47), 27746-27756.

25. Hu, S.-X.; Zhang, P.; Lu, E.; Zhang, P., Decisive Role of 5f-Orbital Covalence in the Structure and Stability of Pentavalent Transuranic Oxo [M_6O_8] Clusters. *Inorganic Chemistry* **2020,** *59* (24), 18068-18077.

Table S1. Optimized geometries (bond length in Å) from PBE/TZ2P and binding energies (Δ*E*, kcal/mol) of Np_2O isomers in different oxidation states from PBE+U, PBE/TZ2P and DLPNO-CCSD(T)/def2-TZVPP (denoted as DLPNO) calculations.

	$^{2S+1}\Lambda$ (Symm.)	Elec. Conf.	*OS* of Np	Structure	Geometry	Δ*E* PBE+U	Δ*E* PBE	Δ*E* DLPNO
1A	$^{11}A_2$ (C_{2v})	f^5s^1-f^5s^1	I	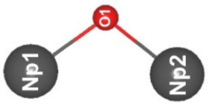	Np–O_b = 2.063 Np1–Np2 = 3.481	0.000	0.000	0.000
1B	$^{13}B_2$ (C_{2v})	f^6-f^5s^1	I	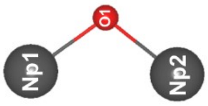	Np–O_b = 2.075 Np1–Np2 =3.087	0.674	0.601	0.568

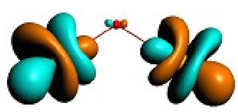

$15b_2$
Np-5f
-2.397

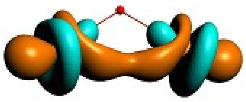

$16a_1$
Np-5f
-2.490

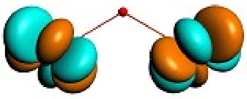

$7a_2$
Np-5f
-2.543

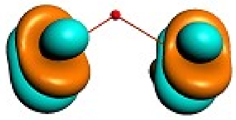

$8b_1$
Np-5f
-2.582

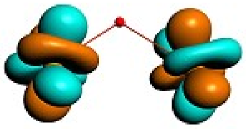

LUMO: $6a_2$
Np-5f
-2.618

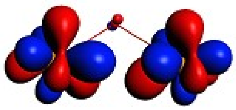

SOMO: $7b_1$
Np-5f
-2.828

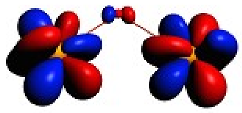

SOMO: $14b_2$
Np-5f
-2.909

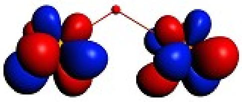

SOMO: $6b_1$
Np-5f
-2.995

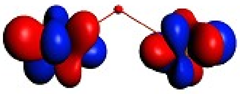

SOMO: $13b_2$
Np-5f
-3.007

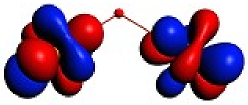

SOMO: $5a_2$
Np-5f
-3.025

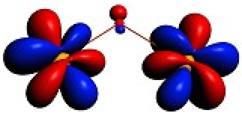

SOMO: $15a_1$
Np-5f
-3.082

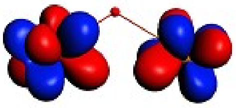

SOMO: $14a_1$
Np-5f
-3.150

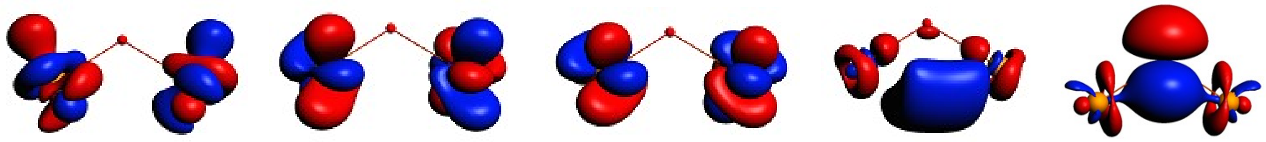

SOMO: $12b_2$
Np-7f
-3.154

SOMO: $11b_2$
Np-5f
-3.310

SOMO: $13a_1$
Np-5f
-3.338

HOMO: $12a_1$
Np-7s
-4.213

HOMO-1:$11a_1$
O-2p
-7.886

Figure S1. Electronic structures of SOMO and bonding–antibonding PBE orbital between O^{2-} and Np for Np_2O.

Table S2. Optimized geometries (bond length in Å) from PBE/TZ2P calculations and binding energies (Δ*E*, kcal/mol) of Np_2O_2 isomers in different oxidation states from PBE+U, PBE/TZ2P and DLPNO-CCSD(T)/def2-TZVPP calculations.

	$^{2S+1}\Lambda$ (Symm.)	Elec. Conf.	*OS* of Np	Structure	Geometry	Δ*E*		
						PBE+U	PBE	DLPNO
2A	$^{11}B_{1g}$ (D_{2h})	$f^4f^5\sigma^1$	II-II	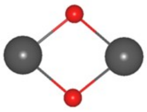	Np–O_b = 2.086 Np1–Np2 = 3.260 O_b1–O_b2 = 2.603	0.000	0.000	0.000
2B	^{11}A (C_1)	f^5s^1-f^3s^1	I-III	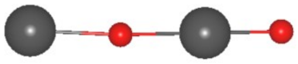	Np1–O_b1 = 2.049 O_b1–Np2 = 2.119 Np2–O_t1 = 1.828	2.608	1.528	2.624

Table S3. Energies and Percent Compositions of the Occupied and Lowest Unoccupied Valence Molecular Orbitals of Np_2O_2.

MO	energy, eV	5f	6d	7s	2p
$7b_{3u}$	-2.18	72.07%	19.91%	8.53%	4.22
$10b_{2u}$	-2.22	54.13%	35.25%	6.61%	2.22%
$6b_{1g}$	-2.364	89.68%	9.70%		
$11a_g$	-2.462	80.12%	11.98%	4.56%	
$9b_{2u}$	-2.539	90.31%	3.40%	9.18%	
LUMO: $3b_{3u}$	-2.577	98.59%			
SOMO+9: $5b_{1g}$	-2.624	97.78%	2.19%		
SOMO+8: $10a_g$	-2.785	90.16%	7.57%		1.99%

SOMO+7: $5b_{3g}$	-2.807	96.98%	2.90%		
SOMO+6: $3b_{2g}$	-2.807	79.58%	18.11%		2.31%
SOMO+5: $8b_{2u}$	-2.903	25.05%	14.06%	44.78%	
SOMO+4: $2a_u$	-2.981	97.25%	2.55%		
SOMO+3: $6b_{1u}$	-2.983	98.26%			0.97%
SOMO+2: $5b_{1u}$	-3.189	88.46%	9.85%		
SOMO+1: $4b_{3g}$	-3.244	98.21%	1.39%		
SOMO: $9a_g$	-3.602	13.89%	13.46%	72.14%	
HOMO:$5b_{3u}$	-7.137	11.21%	2.72%		81.43%

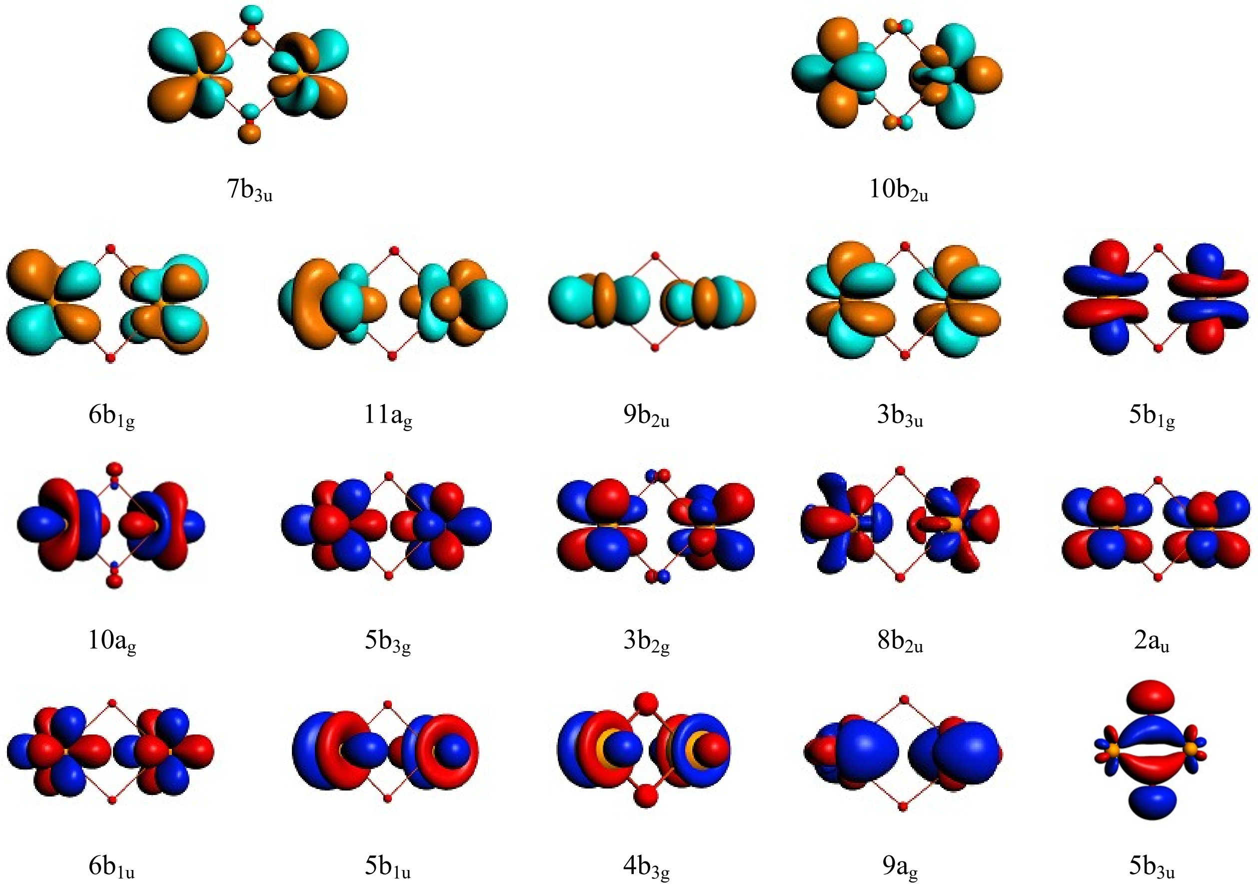

$7b_{3u}$ $10b_{2u}$

$6b_{1g}$ $11a_g$ $9b_{2u}$ $3b_{3u}$ $5b_{1g}$

$10a_g$ $5b_{3g}$ $3b_{2g}$ $8b_{2u}$ $2a_u$

$6b_{1u}$ $5b_{1u}$ $4b_{3g}$ $9a_g$ $5b_{3u}$

Figure S2. Electronic structures of SOMO and Np−O bonding PBE orbitals for Np_2O_2.

Table S4. Optimized geometries (bond length in $\AA$) from PBE/TZ2P and binding energies (ΔE, kcal/mol) of Np_2O_3 isomers in different oxidation states from PBE+U, PBE/TZ2P and DLPNO-CCSD(T)/def2-TZVPP calculations.

$^{2S+1}\Lambda$ (Symm.)	Elec. Conf.	*OS* of Np	Structure	Geometry	ΔE		
					PBE+U	PBE	DLPNO

3A	$^9E''$ (D_{3h})	f^4-f^4	III-III	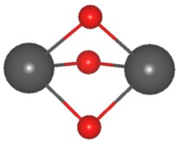	Np–O_b = 2.105 Np1–Np2 = 2.943 O_b–O_b = 2.603	0.000	0.000	0.000
3B	^9A (C_1)	f^4-f^3s^1	II-IV	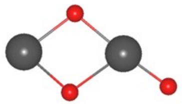	Np1–O = 2.126, 2.011 Np2–O = 2.074, 2197, 1.827 Np1–Np2 = 3.306	1.089	0.341	0.406
3C	^9A (C_1)	f^4-f^4	III-III	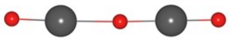	Np1–O = 1.845, 1.994 Np2–O = 2.218, 1.922 Np1–Np2 = 4.304	3.801		

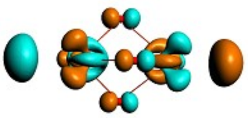

$9a''_2$

Np-7S:66.72%

Np-6D_{z2}:10.61%

Np-5F_x:8.77%

O-2P_z:6.68%

-1.456

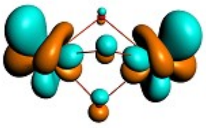

$9e'_{:2}$

Np-5F_{xyz}:36.19%

Np-5F_{z2y}:34.46%

Np-6D_{yz}:11.12%

Np-6D_{xy}:8.92%

O-2P_x:4.88%

-2.033

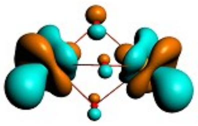

$9e'_{:1}$

Np-5F_z:36.19%

Np-5F_{z2x}:34.46%

Np-6D_{xz}:11.12%

Np-6D_{x2-y2}:8.92%

O-2P_x:2.72%

O-2P_y:2.16%

-2.033

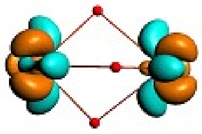

10 a'_1

Np-7S:65.21%

Np-5F_x:12.38%

Np-6D_{z2}:6.45%

Np-5F_{z3}:2.04%

-2.034

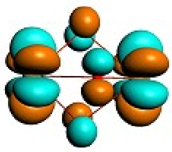

$2a'_2$

Np-5F_y:85.86%

O-2P_x:14.83%

-2.146

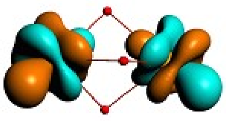

$7e''_{:2}$

Np-5F_z:48.46%

Np-5F_{z2x}:40.42%

Np-6D_{xz}:6.20%

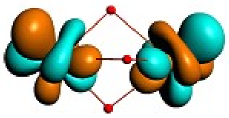

$7e''_{:1}$

Np-5F_{xyz}:48.46%

Np-5F_{z2y}:40.42%

Np-6D_{yz}:6.20%

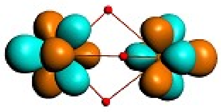

LUMO: $8a''_2$

Np-5F_{z3}:49.58%

Np-5F_x:45.47%

Np-6D_{z2}:5.13%

Np-6D$_{x2-y2}$:4.94%

-2.328

Np-6D$_{xy}$:4.94%

-2.328

Np-7S:1.59%

-2.488

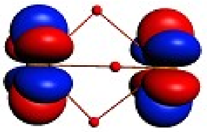

SOMO: 1a$''_1$

Np-5F$_y$:99.66%

Np-6D$_{xz}$:0.33%

-2.709

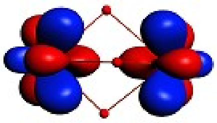

SOMO: 9a$'_1$

Np-5F$_x$:70.04%

Np-5F$_{z3}$:22.03%

Np-7S:6.08%

-2.748

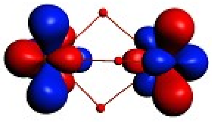

SOMO: 7a$''_2$

Np-5F$_x$:36.82%

Np-5F$_{z3}$:30.59%

Np-6D$_{z2}$:12.35%

Np-7S:5.93%

O-2P$_z$:2.20%

-2.801

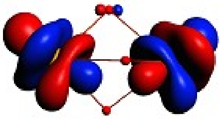

SOMO: 6e$''_{:2}$

Np-5F$_{z2x}$:53.81%

Np-5F$_z$:37.67%

Np-6D$_{x2-y2}$:6.12%

O-2P$_z$:1.31%

Np-6D$_{xz}$:1.03%

-2.848

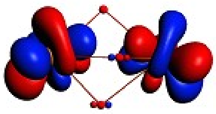

SOMO: 6e$''$:$_1$

Np-5F$_{z2y}$:53.81%

Np-5F$_{xyz}$:37.67%

Np-6D$_{xy}$:6.12%

O-2P$_z$:1.31%

Np-6D$_{yz}$:1.03%

-2.848

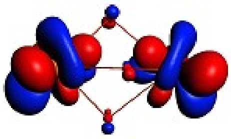

SOMO: 8e$'_{:2}$

Np-5F$_{z2y}$:44.99%

Np-5F$_{xyz}$:41.61%

Np-6D$_{xy}$:6.81%

Np-6D$_{yz}$:3.54%

O-2P$_x$:1.81%

-3.001

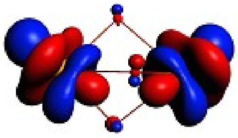

SOMO: 8e$'$:$_1$

Np-5F$_{z2x}$:44.99%

Np-5F$_z$:41.61%

Np-6D$_{x2-y2}$:6.81%

Np-6D$_{xz}$:3.54%

O-2P$_y$:1.81%

-3.001

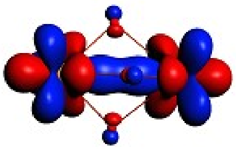

SOMO: 8a$'_1$

Np-5F$_{z3}$:71.19%

Np-5F$_x$:15.65%

Np-7S:9.19%

O-2P$_x$:3.27%

-3.275

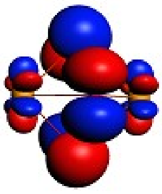

HOMO:1a$'_2$

O-2P$_x$:85.58%

Np-5F$_y$:14.36%

-5.627

Figure S3. Electronic structures of SOMO and Np−O bonding PBE orbital for Np_2O_3.

Table S5. Optimized geometries (bond length in Å) from PBE/TZ2P and binding energies (ΔE, kcal/mol) of Np_2O_4 isomers in different oxidation states from PBE+U, PBE/TZ2P and DLPNOCCSD(T)/ def2-TZVPP calculations.

	$^{2S+1}\Lambda$ (Symm.)	Elec. Conf.	*OS* of Np	Structure	Geometry	ΔE PBE+U	PBE	DLPNO
4A	$^{7}A'$ (C_s)	f^2-f^4	V-III	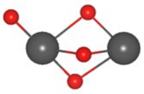	Np1–O = 1.811, 1.972, 2.255, 2.255; Np2–O = 1.997, 2.276, 1.997; Np1–Np2 =2.994	0.000	0.000	0.203
4B	^{7}B (C_2)	f^3-f^3	IV	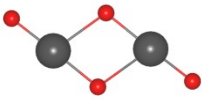	Np–O = 1.818, 2.256, 1.972; Np1–Np2 =3.373	0.713	0.134	1.544
4C	^{7}A (C_i)	f^3-f^3	IV	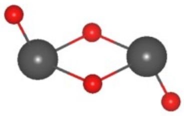	Np–O = 1.816, 2.270, 1.966; Np1–Np2 =3.368	0.728	0.086	0.000
4D	$^{7}A_2$ (C_{2v})	f^3-f^3	IV	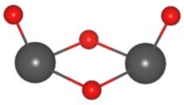	Np–O = 1.836, 2.098, 2.098; Np1–Np2 =3.331	0.795	0.563	0.343

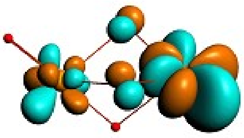	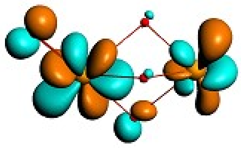	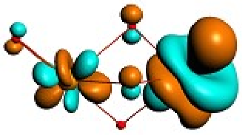	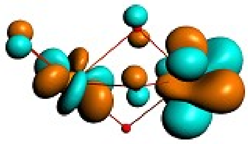
19a'' Np-5F_{z3}:49.50% Np-5F_{z}:9.56% Np-5F_{xyz}:16.68% Np-6D_{xz}:8.60% O-2P_{z}:6.09%	35a' Np-5F_{x}:37.15% Np-5F_{y}:28.74% Np-7S:6.36% O-2P_{y}:6.17% O-2P_{x}:4.14%	34a' Np-5F_{x}:36.40% Np-5F_{y}:21.54% Np-5F_{z2x}:16.97% Np-5F_{z2y}:7.08% Np-6D_{x2-y2}:5.47%	18a'' Np-5F_{z}:57.29% Np-5F_{z3}:15.56% Np-5F_{xyz}:9.38% Np-6D_{xz}:7.06% O-2P_{y}:4.17%

Np-6D$_{yz}$:3.59% -2.651	Np-6D$_{x2-y2}$:3.78% Np-6D$_{xy}$:1.01% -2.661	O-2P$_{y}$:4.32% Np-6D$_{z2}$:3.72% Np-6D$_{xy}$:2.27% -2.755	O-2P$_{z}$:2.56% Np-6D$_{yz}$:2.12% -2.758
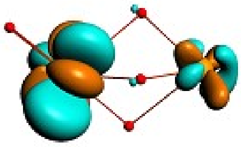	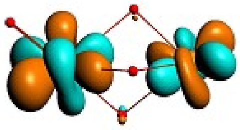	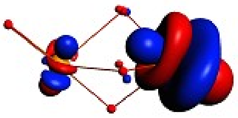	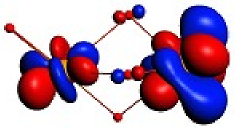
33a' Np-5F$_{z2y}$:59.81% Np-5F$_{z2x}$:24.55% Np-5F$_{x}$:2.81% Np-6D$_{z2}$:2.50% Np-7S:4.24% -3.064	LUMO: 17a'' Np-5F$_{z}$:61.30% Np-5F$_{z3}$:18.88% Np-5F$_{xyz}$:13.95% Np-6D$_{xz}$:1.83% Np-6D$_{yz}$:1.07% -3.206	SOMO: 32a' Np-5F$_{y}$:50.86% Np-5F$_{z2x}$:24.51% Np-5F$_{z2y}$:9.12% Np-6D$_{z2}$:5.05% Np-6D$_{xy}$:2.67% Np-5F$_{x}$:3.24% -3.384	SOMO: 16a'' Np-5F$_{xyz}$:67.81% Np-5F$_{z3}$:13.19% Np-6D$_{yz}$:8.06% Np-5F$_{z}$:5.81% O-2P$_{x}$:1.96% Np-6D$_{xz}$:1.38% -3.397
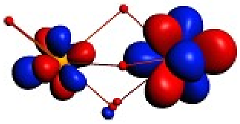	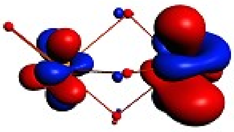	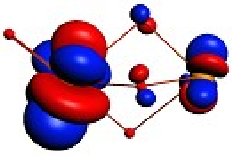	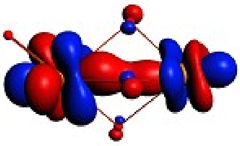
SOMO: 31a' Np-5F$_{z2y}$:50.86% Np-5F$_{x}$:24.51% Np-5F$_{z2x}$:9.12% Np-5F$_{y}$:24.51% -3.479	SOMO: 30a' Np-5F$_{z2y}$:49.56% Np-5F$_{y}$:24.40% Np-7S:5.10% Np-5F$_{x}$:3.98% Np-5F$_{z2x}$:4.47% Np-6D$_{xy}$:2.05% O-2P$_{x}$:1.43% -3.602	SOMO: 15a'' Np-5F$_{z3}$:40.33% Np-5F$_{z}$:29.65% Np-5F$_{xyz}$:24.71% O-2P$_{y}$:1.70% -3.734	SOMO: 29a' Np-5F$_{z2x}$:53.66% Np-5F$_{x}$:24.68% Np-5F$_{y}$:11.32% Np-5F$_{z2y}$:4.03% O-2P$_{z}$:2.46% Np-7S:1.77% -4.054
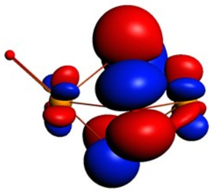			
HOMO:14a''			

O-2P$_y$:48.53% O-2P$_z$:32.41% Np-5F$_{z3}$:8.32% O-2P$_x$:3.34% Np-5F$_z$:4.70% -6.261			

Figure S4. Electronic structures of SOMO and Np−O bonding PBE orbital for Np_2O_4.

Table S6. Optimized geometries (bond length in Å) from PBE/TZ2P and binding energies (Δ*E*, kcal/mol) of Np_2O_5 isomers in different oxidation states from PBE+U, PBE/TZ2P and DLPNOCCSD(T)/ def2-TZVPP calculations.

	$^{2S+1}\Lambda$ (Symm.)	Elec. Conf.	*OS* of Np	Structure	Geometry	Δ*E* PBE+U	PBE	DLPNO
5A	^5A (C_2)	f^2-f^2	V	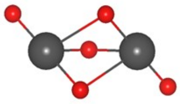	Np1−O$_t$1,O$_b$1,O$_b$2,O$_b$3 = 1.802, 2.103, 2.444, 1.899 Np1−Np2 = 3.105	0.000	0.000	0.000
5B	^5A (C_2)	f^2-f^2	V	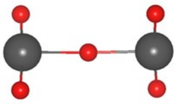	Np1−O$_t$1,O$_t$2,O$_b$1 = 1.807, 1.808, 2.809; Np1−Np2 =4.173	0.630	0.739	0.948
5C				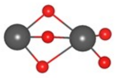	Np1−O = 2.060, 2.060, 1.962; Np2−O = 2.202, 2.190, 2.418, 1.847, 1.849; Np1−Np2 =3.049	2.349		
5D				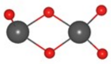	Np1-O = 1.871, 2.138, 2.135; Np2-O = 2.085, 2.090, 1.840, 1.839; Np1-Np2 = 3.348	2.301		
5E				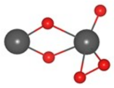	Np1-O=2.023,2.013; Np2-O=2.262,2.334,	3.841		

		1.845, 2.218, 2.050; Np1-Np2 =3.345 O-O=1.471	
5F	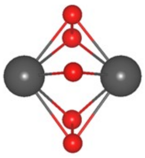	Np-O = 2.376, 2.400, 2.147, 2.326, 2.438; Np1-Np2 =2.859 O-O=1.490	6.584

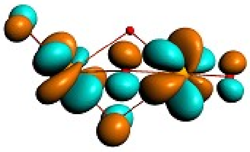	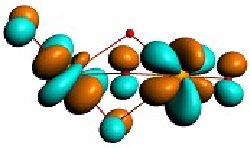	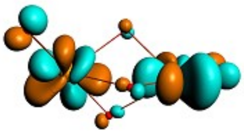	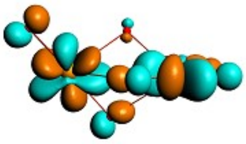
29b Np-5F$_{z2x}$:31.93% Np-5F$_{z2y}$:18.05% Np-5F$_{y}$:11.63% O-2P$_{z}$:8.47% Np-5F$_{z}$:5.42% -2.166	29a Np-5F$_{z2y}$:25.31% Np-5F$_{z2x}$:19.17% Np-5F$_{y}$:12.43% Np-5F$_{z}$:7.52% O-2P$_{z}$:11.82% -2.902	28b Np-5F$_{x}$:19.61% Np-5F$_{y}$:17.34% Np-7S:11.28% Np-5F$_{z}$:10.73% Np-5F$_{z2y}$:6.85% O-2P$_{x}$:4.38% -2.986	28a Np-5F$_{x}$:31.59% Np-5F$_{y}$:14.86% Np-5F$_{z}$:12.92% Np-5F$_{xyz}$:5.65% O-2P$_{y}$:8.19% Np-5F$_{z2x}$:4.51% -3.095
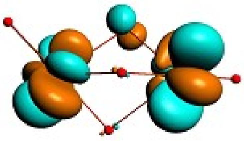	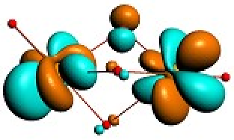	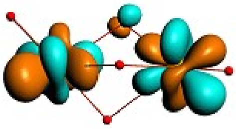	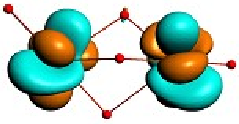
27b Np-5F$_{z3}$:29.06% Np-5F$_{xyz}$:23.27% Np-5F$_{z2x}$:21.34% Np-5F$_{z2y}$:8.54% Np-6D$_{xz}$:3.85% O-2P$_{x}$:3.44% -3.425	27a Np-5F$_{z3}$:30.73% Np-5F$_{z}$:15.88% Np-5F$_{xyz}$:13.50% Np-5F$_{x}$:7.61% Np-5F$_{z2x}$:6.90% Np-6D$_{yz}$:5.13% Np-5F$_{y}$:4.97% -3.431	26b Np-5F$_{z}$:42.63% Np-5F$_{x}$:30.04% Np-5F$_{z3}$:10.07% Np-5F$_{z2y}$:5.49% Np-6D$_{z2}$:2.17% O-2P$_{x}$:1.70% -3.699	LUMO: 26a Np-5F$_{z}$:35.18% Np-5F$_{z2x}$:22.00% Np-5F$_{x}$:18.69% Np-5F$_{xyz}$:11.65% Np-5F$_{z3}$:8.89% -3.770

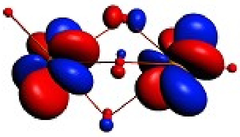	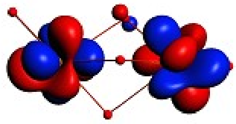	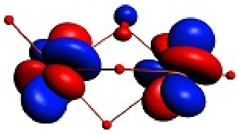	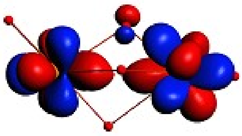
SOMO: 25b Np-5F$_{z2y}$:32.57% Np-5F$_{z3}$:23.98% Np-5F$_{z2x}$:23.94% Np-5F$_{xyz}$:9.68% Np-6D$_{z2}$:2.45% -4.153	SOMO: 24b Np-5F$_{y}$:36.97% Np-5F$_{z}$:23.78% Np-5F$_{z3}$:14.23% Np-5F$_{xyz}$:7.22% Np-5F$_{z2y}$:6.85% Np-5F$_{x}$:4.94% Np-5F$_{z2x}$:1.52% -4.328	SOMO: 25a Np-5F$_{z2y}$:37.42% Np-5F$_{z2x}$:35.72% Np-5F$_{z3}$:15.63% Np-5F$_{xyz}$:5.39% Np-5F$_{z}$:1.67% -4.429	SOMO: 24a Np-5F$_{y}$:36.77% Np-5F$_{z3}$:19.18% Np-5F$_{x}$:13.47% Np-5F$_{z2y}$:12.17% Np-5F$_{xyz}$:5.66% Np-5F$_{z}$:5.55% Np-5F$_{z2x}$:3.33% -4.547
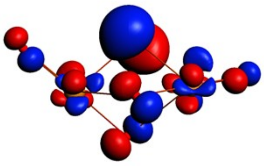			
HOMO:23b O-2P$_{x}$:49.12% O-2P$_{y}$:17.69% O-2P$_{z}$:11.86% Np-5F$_{y}$7.20% Np-5F$_{z2x}$:4.98% -6.566			

Figure S5. Electronic structures of SOMO and bonding−antibonding PBE orbital between O^{2-} and Np for Np_2O_5.

Table S7. Optimized geometries (bond length in Å) from PBE/TZ2P and binding energies (Δ*E*, kcal/mol) of Np_2O_6 isomers in different oxidation states from PBE+U, PBE/TZ2P and DLPNOCCSD(T)/ def2-TZVPP calculations.

${}^{2S+1}\Lambda$ (Symm.)	Elec. Conf.	*OS* of Np	Structure	Geometry	Δ*E*		
					PBE+U	PBE	DLPNO

6A	$^3B_{2u}$ (D_{2h})	f^1-f^1	VI-VI	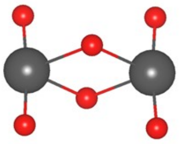	Np–O = 2.100, 2.100, 1.792, 1.792 Np1–Np2 = 3.323	0.000	0.092	0.000
6B	$^3B_2$ (C_{2v})	f^2-f^0	V-VII	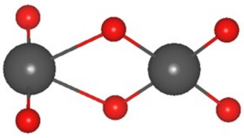	Np1–O = 1.955, 1.816; Np2–O = 2.266, 1.797; Np1–Np2 =3.363	0.101	0.000	2.425
6C	$^1A'$ (C_s)	f^2-f^0	V-VII	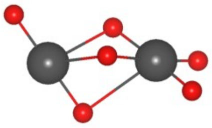	Np1–O = 1.817, 1.817, 1.985, 1.985, 3.828; Np2–O = 1.790, 1.789, 2.215, 2.215 Np1–Np2 = 3.347	1.117	0.222	2.981
6D	$^5A'$ (C_s)	f^2-f^2	V-V	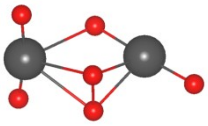	Np2–O = 1.810, 1.810, 2.394, 2.413, 2.390; Np1–O =1.889,2.259, 2.259, 1.798; Np1–Np2 = 3.456	1.348	2.669	2.409
6E	^3A (C_1)	f^3-f^1	V-V	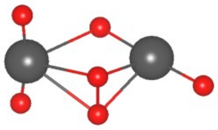	Np2–O = 1.805, 1.805, 2.360, 2.357, 2.362; Np2–O = 2.288, 1.910, 2.291, 1.806; Np1–Np2 =3.417	1.729	2.939	-

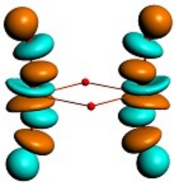	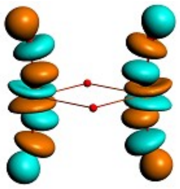	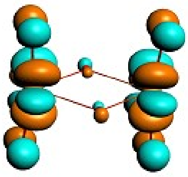	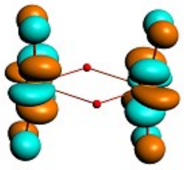
9b$_{2u}$ O-2P$_y$:40.63%	8b$_{3g}$ O-2P$_y$:39.70%	8b$_{3u}$ Np-5F$_x$:71.49%	7b$_{2g}$ Np-5F$_x$:67.00%

Np-5F$_{y}$:22.68% Np-5F$_{z2y}$:13.69% O-2P$_{z}$:8.67% -0.148	Np-5F$_{y}$:23.07% Np-5F$_{z2y}$:13.16% O-2P$_{z}$:7.48% -0.153	O-2P$_{x}$:24.62% -3.298	O-2P$_{x}$:21.63% Np-6D$_{xz}$:6.55% Np-5F$_{z2x}$:1.48% -3.342
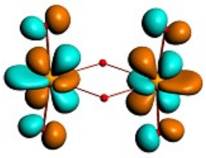	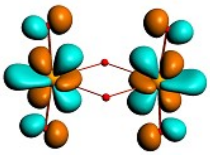	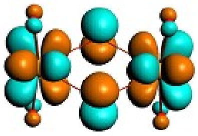	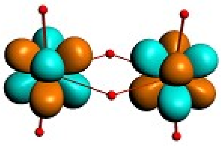
12b$_{1u}$ Np-5F$_{z}$:39.52% Np-5F$_{z3}$:19.65% O-2P$_{z}$:16.45% Np-7S:16.26% O-2P$_{y}$:4.73% Np-6D$_{z2}$:2.73% -3.466	13a$_{g}$ Np-5F$_{z}$:36.85% Np-5F$_{z3}$:22.75% O-2P$_{z}$:17.85% Np-7S:7.92% O-2P$_{y}$:4.12% Np-6D$_{z2}$:4.02% -3.532	4b$_{1g}$ Np-5F$_{xyz}$:76.90% O-2P$_{y}$:18.41% O-2P$_{x}$:4.75% -4.037	7b$_{3u}$ Np-5F$_{z2x}$:73.70% Np-6D$_{xz}$:12.74% O-2P$_{x}$:11.38% -4.056
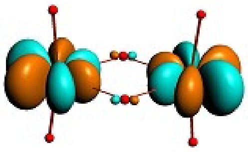	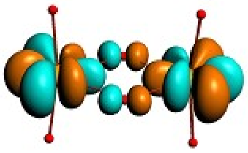	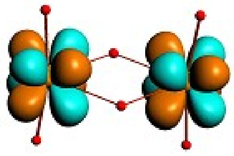	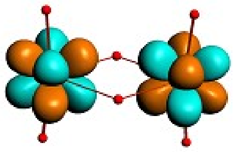
6b$_{2g}$ Np-5F$_{z2x}$:87.82% Np-6D$_{xz}$:5.76% Np-5F$_{x}$:4.11% O-2P$_{z}$:1.48% -4.594	11b$_{1u}$ Np-5F$_{z3}$:54.90% Np-5F$_{z}$:24.05% O-2P$_{z}$:8.61% Np-6D$_{z2}$:5.15% Np-6D$_{x2-y2}$:4.32% -4.627	3a$_{u}$ Np-5F$_{xyz}$:97.96% O-2P$_{x}$:0.82% -4.794	LUMO: 7b$_{3g}$ Np-5F$_{z2y}$:62.11% Np-5F$_{y}$:35.29% O-2P$_{z}$:1.46% -4.946
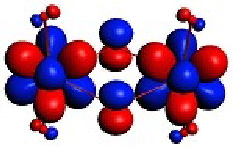	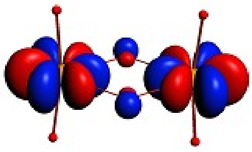	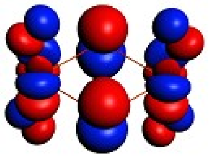	
SOMO: 8b$_{2u}$ Np-5F$_{z2y}$:60.20% Np-5F$_{y}$:26.44% O-2P$_{y}$:10.27%	SOMO: 12a$_{g}$ Np-5F$_{z3}$:58.13% Np-5F$_{z}$:33.90% O-2P$_{x}$:3.46%	HOMO:7b$_{2u}$ O-2P$_{y}$:62.55% Np-5F$_{y}$:26.02% O-2P$_{z}$:7.05%	

O-2P$_z$:2.41% -5.015	Np-6D$_{z2}$:1.38% Np-6D$_{x2-y2}$:1.26% -5.097	-6.105	

Figure S6. Electronic structures of SOMO and bonding–antibonding PBE orbital between O^{2-} and Np for Np$_2$O$_6$.

Table S8. Optimized geometries (bond length in Å) from PBE/TZ2P and binding energies (Δ*E*, kcal/mol) of Np$_2$O$_7$ isomers in different oxidation states from PBE+U, PBE/TZ2P and DLPNOCCSD(T)/ def2-TZVPP (DLPNO) calculations.

	$^{2S+1}\Lambda$ (Symm.)	Elec. Conf.	*OS* of Np	Structure	Geometry	Δ*E*		
						PBE+U	PBE	DLPNO
7A	^{1}A′ (C_s)	f^0-f^0	VII-VII	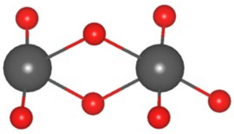	Np1–O$_t$1,O$_t$2,O$_b$1,O$_b$2 = 1.787, 1.787, 2.013, 1.961; Np2–O$_b$1,O$_b$2,O$_t$4,O$_t$5,O$_t$3 = 2.236, 2.324, 1.797, 1.797, 1.846; Np1–Np2 = 3.493	0.000	0.000	0.000
7B	^{3}A’ (C_s)	(O$_{2p}$)^1-f^1	VI-VII	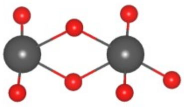	Np1–O$_t$1,O$_t$2,O$_b$1,O$_b$2 = 1.784, 1.784, 2.015, 2.105; Np2–O$_b$1,O$_b$2,O$_t$4,O$_t$5 = 2.095, 2.233, 1.804, 1.804; Np1–Np2 = 3.400	0.055	0.719	1.410
7C	^{3}A (C_1)	f^1-f^1	VI-VI	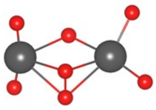	Np1–O$_t$1,O$_t$2,O$_b$1,O$_b$2,O$_b$3 = 1.794, 1.797, 2.246, 2.310, 2.312; Np2–O$_b$1,O$_b$2,O$_b$3,O$_t$4,O$_t$3 = 1.955, 2.363, 2.353, 1.836, 1.803 Np1–Np2 = 3.442	0.460	1.532	1.282
7D	^{1}A (C_1)	f^1-f^1	VI-VI	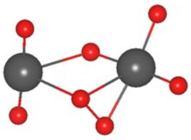	Np2–O$_t$1,O$_t$2,O$_b$1,O$_b$2,O$_b$3 = 1.793, 1.796, 2.199, 2.282, 2.286; Np1–O$_b$1,O$_b$2,O$_b$3,O$_t$4,O$_t$3 = 1.985, 2.394, 2.395, 1.834, 1.806; Np1–Np2 = 3.435	0.496	1.546	1.647

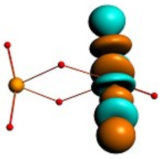	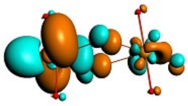	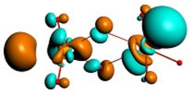	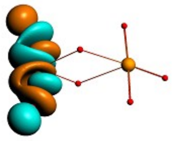	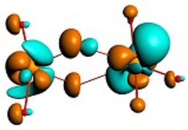
25a" O-2P$_z$:50.34% Np-5F$_{z3}$:39.30% O-2P$_y$:3.74% Np-6D$_{yz}$:1.80% Np-6D$_{xz}$:1.39% -0.189	46a' Np-6D$_{x2\text{-}y2}$:6.54% Np-7S:6.54% O-2P$_x$:17.21% O-2P$_y$:5.33% Np-5F$_{z2x}$:75.16% -0.685	45a' Np-7S:49.61% Np-6D$_{x2\text{-}y2}$:16.52% Np-6D$_{xy}$:5.76% Np-5F$_{z2x}$:3.89% O-2P$_x$:3.38% O-2P$_y$:2.64% Np-6D$_{z2}$:2.49% Np-5F$_{z2y}$:1.10% -0.986	24a" Np-5F$_{z3}$:37.34% O-2P$_z$:32.86% O-2P$_x$:13.81% Np-6D$_{xz}$:7.19% Np-7S:1.44% -1.557	44a' Np-7S:56.06% O-2P$_x$:4.43% Np-6D$_{z2}$:5.68% Np-6D$_{x2\text{-}y2}$:4.87% Np-5F$_{z2x}$:4.91% Np-6D$_{xy}$:3.25% Np-5F$_{z2y}$:2.82% Np-5F$_y$:1.34% Np-5F$_x$:1.26% -1.718
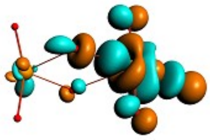	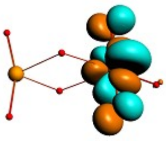	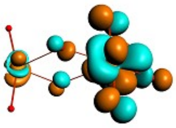	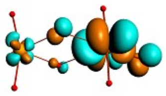	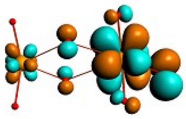
43a' Np-5F$_{z2x}$:21.37% Np-5F$_y$:18.39% Np-5F$_{z2y}$:16.82% O-2P$_x$:15.13% O-2P$_y$:8.44% Np-7S:5.27% Np-6D$_{x2\text{-}y2}$:3.14% O-2P$_z$:1.68% -2.744	42a' Np-5F$_{z2y}$:36.31% Np-5F$_{z2x}$:32.41% O-2P$_y$:11.75% O-2P$_x$:10.54% Np-7S:3.58% Np-6D$_{x2\text{-}y2}$:1.21% Np-6D$_{xy}$:1.03% -3.317	41a' Np-5F$_y$:37.88% Np-5F$_{z2y}$:15.27% Np-5F$_{z2x}$:14.30% O-2P$_x$:13.44% O-2P$_y$:10.07% Np-5F$_x$:2.92% -3.947	40a' Np-5F$_x$:72.54% O-2P$_y$:7.83% Np-5F$_y$:2.77% O-2P$_x$:2.02% Np-5F$_{z2x}$:1.89% Np-6D$_{xy}$:1.79% Np-6D$_{x2\text{-}y2}$:1.36% Np-7S:1.33% -4.236	23a" Np-5F$_{xyz}$:70.27% O-2P$_z$:17.65% Np-5F$_z$:6.30% O-2P$_x$:2.58% -4.307
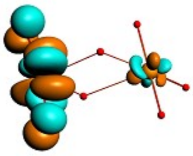	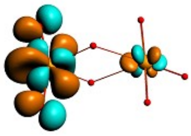	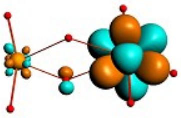	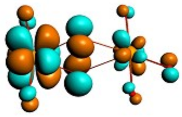	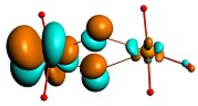

39a' Np-5F_{z2y}:66.63% O-2P_y:22.46% Np-5F_y:4.61% Np-6D_{xy}:2.93% -4.426	38a' Np-5F_{z2x}:57.09% O-2P_x:13.45% Np-7S:9.86% O-2P_z:7.95% Np-5F_x:5.53% Np-6D_{x2-y2}:1.33% -4.625	22a'' Np-5F_z:88.53% Np-5F_{xyz}:8.48% O-2P_z:1.36% -5.282	21a'' Np-5F_{xyz}:75.16% O-2P_z:17.21% O-2P_y:5.33% -5.282	37a' Np-5F_y:70.25% Np-6D_{xy}:9.58% O-2P_y:12.55% Np-5F_{z2y}:1.93% Np-5F_x:1.06% -5.399
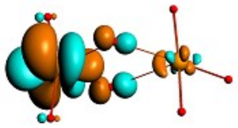	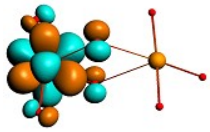	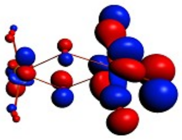	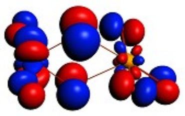	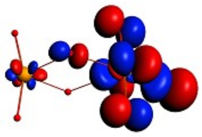
36a' Np-5F_x:74.97% Np-6D_{x2-y2}:6.54% O-2P_x:8.19% Np-5F_{z2x}:2.28% Np-5F_y:1.23% -5.647	LUMO:20a'' Np-5F_z:86.23% O-2P_z:7.89% O-2P_x:3.03% -5.793	HOMO:19a'' O-2P_z:54.02% Np-5F_{z3}:19.55% Np-5F_{xyz}:12.91% Np-5F_z:4.38% O-2P_y:2.10% O-2P_x:1.21% -6.594	18a'' O-2P_z:57.73% O-2P_x:17.39% Np-5F_{z3}:10.18% Np-5F_z:7.16% Np-5F_{xyz}:3.10% O-2P_y:1.54% -7.078	35a' O-2P_x:43.14% Np-5F_y:23.56% O-2P_y:18.98% Np-5F_x:2.25% Np-6D_{xy}:1.15% -7.083
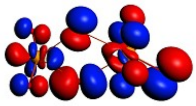	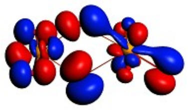	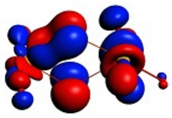	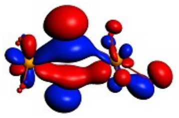	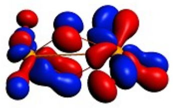
34a' O-2P_x:43.80% O-2P_y:37.85% Np-6D_{x2-y2}:4.83% Np-5F_x:5.22% Np-5F_{z2y}:1.78% Np-5F_x:5.22% -7.993	33a' O-2P_y:40.24% O-2P_x:34.23% Np-5F_x:8.96% Np-5F_y:2.31% O-2P_z:1.54% -8.137	17a'' O-2P_z:46.27% Np-5F_{xyz}:14.30% O-2P_y:16.23% Np-5F_{z3}:14.74% O-2P_x:3.08% -8.273	32a' O-2P_y:66.55% Np-5F_y:15.05% O-2P_x:6.10% Np-5F_x:2.96% O-2P_z:1.05% -8.558	16a'' O-2P_z:43.61% O-2P_x:20.44% Np-5F_{z3}:17.93% Np-5F_{xyz}:9.94% O-2P_y:3.37% Np-6D_{xz}:1.47% -8.741

Figure S7. Electronic structures of SOMO and Np−O bonding PBE orbitals for Np_2O_7.

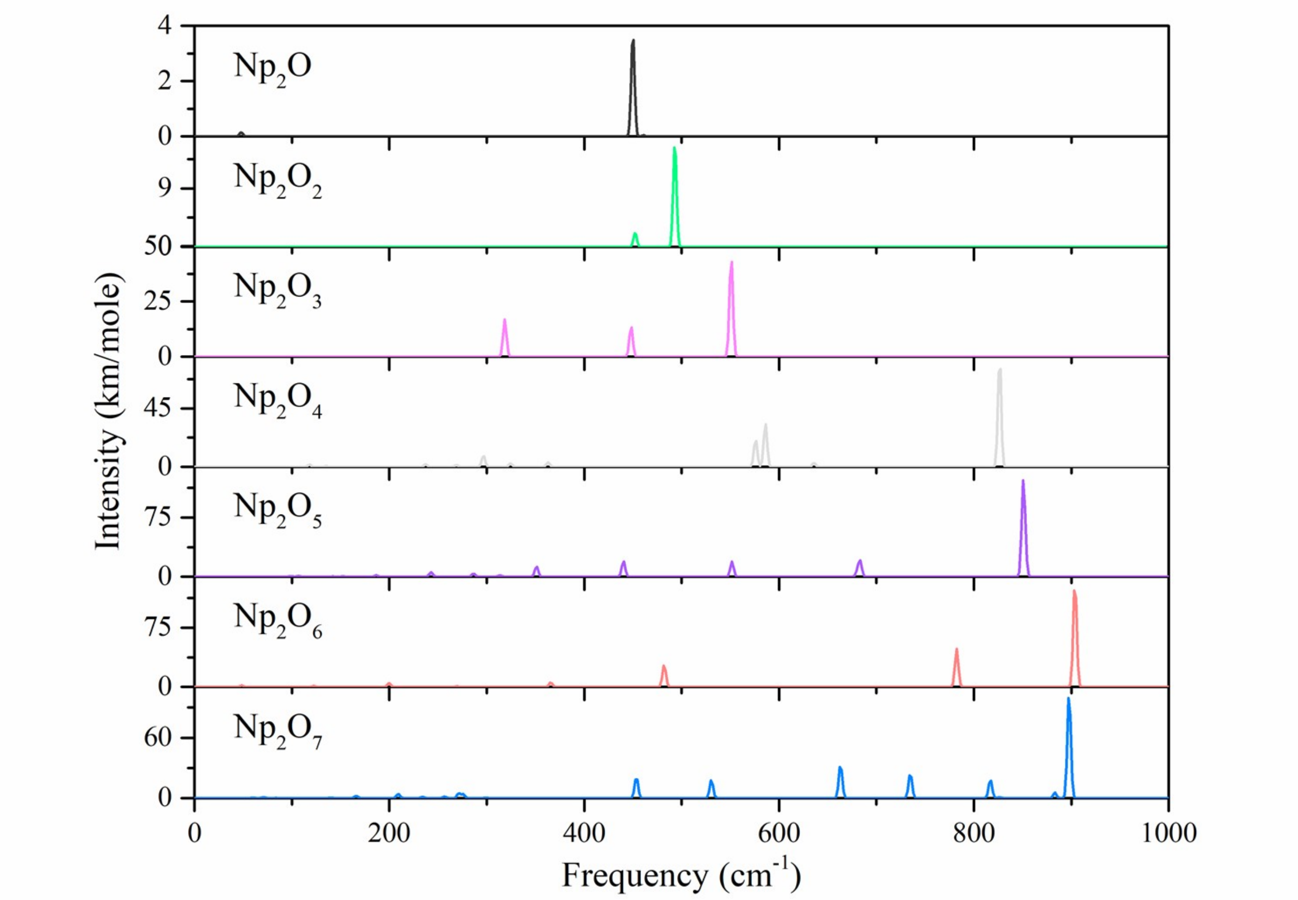

Figure S8. DFT computed spectrum of the lowest-energy isomer for [Np_2O_x] species. None scaled.

Table S9. Calculated bond orders of Np-Np and Np-O in Np_2O_x molecules.

	Mayer	G-J	N-M (1)	N-M (2)	N-M (3)
Np_2O					
Np1-Np2	1.51	1.55	3.88	3.81	3.77
Np-O$_b$	0.93	1.25	2.28	2.31	2.34
Np_2O_2					
Np1-Np2	0.77	0.85	2.04	1.78	1.92
Np-O$_b$	0.93	1.20	2.14	2.26	2.17
O$_b$1-O$_b$2	0.01	0.03	0.03	-0.18	0.04
Np_2O_3					
Np1-Np2	0.55	0.74	1.50	0.87	1.37
Np-O$_b$	0.93	1.17	1.86	2.08	1.88

O_b-O_b	0.00	0.03	0.03	-0.21	0.04
Np_2O_4					
Np1-O_t1	2.01	2.41	3.09	3.16	3.07
Np1-O_b1	1.29	1.60	2.07	2.29	2.11
Np1-O_b2	0.63	0.79	1.03	1.34	1.06
Np1-O_b3	0.63	0.79	1.03	1.34	1.06
Np2-O_b1	1.25	1.57	2.33	2.52	2.35
Np2-O_b2	0.56	0.71	1.06	1.33	1.06
Np2-O_b3	1.25	1.57	2.33	2.52	2.35
Np1-Np2	0.72	0.92	1.51	0.73	1.37
Np_2O_5					
Np1-O_t1	0.01	0.02	0.03	0.26	0.03
Np1-O_b1	0.93	1.18	1.56	1.83	1.59
Np1-O_b2	1.51	1.89	2.48	2.64	2.49
Np1-O_b3	0.38	0.46	0.60	0.88	0.60
Np1-Np2	0.31	0.44	0.66	-0.14	0.60
Np_2O_6					
Np1-O_t1	0.92	1.20	1.39	1.65	1.43
Np1-O_t2	0.92	1.20	1.39	1.65	1.43
Np1-O_b1	0.02	0.03	0.03	0.23	0.03
Np1-O_b2	0.02	0.03	0.03	0.23	0.03
Np1-Np2	1.02	1.12	1.38	0.53	1.26
Np2O7					
Np1-O_t1	0.01	0.02	0.02	0.16	0.02
Np1-O_t2	0.01	0.02	0.02	0.16	0.02
Np1-O_b1	0.63	0.79	0.90	1.12	0.92
Np1-O_b2	0.45	0.60	0.69	0.90	0.70
Np2-O_b1	1.27	1.65	1.89	2.07	1.91
Np2-O_b2	1.50	1.90	2.18	2.33	2.20
Np2-O_t4	0.03	0.05	0.05	0.23	0.05
Np2-O_t5	0.03	0.05	0.05	0.23	0.05
Np2-O_t3	0.04	0.04	0.05	0.24	0.05

Np1-Np2	0.13	0.19	0.24	-0.45	0.22

Table S10. Charge analyses on Np and O atoms of Np_2O molecules.

Atom	Bader charge	Mulliken Charge	Mulliken Spin
Np_2O			
Np1/Np2	0.63	0.46	5.45
O_b	-1.27	-0.92	-0.14
Np_2O_2			
Np1/Np2	1.20	0.91	5.14
O_b1/O_b2	-1.2	-0.91	-0.14
Np_2O_3			
Np1/Np2	1.75	1.33	4.16
$O_b1/O_b2/O_b3$	-1.16	-0.89	-0.11
Np_2O_4			
Np1	2.39	1.73	2.35
Np2	1.77	1.43	3.92
O_t1	-1.01	-0.64	-0.13
O_b1	-0.88	-0.83	-0.10
O_b2/O_b3	-1.13	-0.85	-0.11
Np_2O_5			
Np1/Np2	2.42	1.82	2.23
O_b1	-1.1	-0.87	-0.06
O_t1/O_t2	-0.99	-0.62	-0.11
O_b2/O_b3	-0.88	-0.77	-0.09
Np_2O_6			
Np1/Np2	2.62	2.05	1.15
O_b1/O_b2	-1.04	-0.87	-0.04
$O_t1/O_t2/O_t3/O_t4$	-0.79	-0.59	-0.06
Np_2O_7			
Np1	2.74	2.24	0.00
Np2	2.79	2.15	0.00
O_b1	-0.91	-0.8	0.00

O_b2	-0.9	-0.78	0.00
O_t5	-0.75	-0.57	0.00
O_t1/O_t2	-0.78	-0.55	0.00
O_t3/O_t4	-0.71	-0.57	0.00

Table S11 PBE+U Cartisian for Np_2O_x (x=1 to 7)

3

1A

Np	5.268953	4.927047	5.273626
Np	5.513628	8.262416	5.336709
O	6.039968	6.525677	6.392654

3

1B

Np	5.259178	4.981862	5.251232
Np	5.497646	8.210257	5.312237
O	6.065724	6.523021	6.439519

4

2A

Np	12.519278	12.761116	10.823786
Np	10.298797	10.328843	11.028972
O	11.517529	11.567084	12.269841
O	11.270728	11.550755	9.585636

4

2B

Np	12.547102	11.739142	11.082000
Np	9.810308	10.457256	14.043201
O	8.524985	9.896086	15.261621
O	11.230405	11.086998	12.690873

5

3A

Np	9.826376	11.534555	13.747706
Np	11.274442	12.355656	11.304026

O	9.910345	13.374035	12.621064
O	9.826373	10.813752	11.715089
O	11.915188	11.646460	13.241349

5

3B

Np	5.277650	4.494049	5.505849
Np	6.448528	7.450982	6.551682
O	4.745936	6.481439	5.504059
O	6.953129	5.392665	6.513955
O	6.101178	9.287185	6.651777

5

3C

Np	12.610426	11.771232	11.003878
Np	9.828362	10.468286	14.018701
O	8.556658	9.908863	15.232691
O	11.207862	11.074543	12.712801
O	13.764463	12.295634	9.559175

6

4A

Np	9.881228	10.520100	6.062859
Np	11.127924	8.135601	4.651104
O	9.050376	9.375203	4.769067
O	10.705466	8.508757	6.637641
O	11.580351	10.150605	4.645251
O	10.641171	11.622578	7.279519

6

4B

Np	5.846002	6.511973	6.336882
Np	5.660830	7.887699	9.481335
O	5.771096	8.321464	7.233081
O	5.925743	4.864904	5.481683
O	5.605391	9.533253	10.341741
O	5.727348	6.078861	8.584607

6

4C

Np	6.978400	5.729613	5.452394
Np	5.770552	7.443964	8.042505
O	5.153270	6.170863	6.447005
O	7.493310	3.994481	5.967753
O	7.594130	7.005725	7.045427
O	5.263764	9.184629	7.538511

6

4D

Np	6.787081	5.478073	6.041691
Np	7.166871	8.799111	6.045771
O	6.271142	7.217402	7.161874
O	5.281525	4.936596	5.055812
O	7.792636	7.046887	5.005282
O	5.826207	9.679579	5.065109

7

5A

Np	5.420527	7.084193	6.166913
Np	8.494209	6.525589	6.021966
O	9.376044	5.460608	4.870796
O	7.597431	7.630122	7.246644
O	6.975341	7.264647	4.711316
O	4.567759	8.639997	5.871322
O	6.290019	5.453249	6.500138

7

5B

Np	5.368548	8.260140	6.382028
Np	7.307525	4.482440	6.317128
O	6.350411	6.378993	6.366280
O	7.212458	4.409525	4.529082
O	6.915628	9.139664	6.155065
O	3.762259	7.496448	6.608470

O	7.454918	4.444507	8.103258

8

6A

Np	11.791632	11.791497	13.313937
Np	11.791449	11.791621	9.961376
O	12.335850	10.595712	11.642278
O	11.246789	12.987247	11.642208
O	13.403308	12.516091	9.857506
O	10.179854	11.066989	9.857454
O	10.196259	11.053419	13.393697
O	13.386981	12.529782	13.392433

8

6B

Np	5.301410	7.201695	5.615735
Np	8.541425	6.303755	6.220517
O	8.732321	5.622178	4.582781
O	8.416636	6.966615	7.873243
O	7.035723	7.958648	5.416738
O	4.505810	8.694684	4.980487
O	6.244692	5.685532	6.270168
O	3.703695	6.386041	5.843537

8

6C

Np	5.401073	7.122486	6.156325
Np	8.505576	6.509779	6.083351
O	9.200246	5.355886	4.917882
O	7.794271	7.690828	7.279812
O	6.771813	7.454983	4.809978
O	4.553448	8.691538	5.655944
O	6.443850	5.501764	6.508184
O	4.200688	6.617040	7.465716

8

6D

Np	12.407861	10.909637	10.905654
Np	12.245913	10.616317	14.384233
O	11.404913	11.427911	9.510952
O	11.710389	8.898813	14.359475
O	12.934129	12.250542	14.686022
O	11.271259	11.988803	12.500194
O	10.775160	10.571832	12.419849
O	13.526176	10.356021	12.295517

8

6E

Np	12.409327	10.917677	10.905169
Np	12.247190	10.616301	14.382742
O	11.398760	11.420240	9.514847
O	11.706403	8.900255	14.358411
O	12.941063	12.248178	14.686759
O	11.269138	11.979671	12.517998
O	10.774138	10.562880	12.406384
O	13.529779	10.374672	12.289588

9

7A

Np	13.174581	10.970499	11.889051
Np	9.964685	11.696744	10.983307
O	9.805771	12.902048	12.245306
O	14.185205	9.815660	13.027204
O	11.042712	10.422121	12.238461
O	13.129046	12.202065	13.177073
O	9.981103	10.524256	9.681215
O	12.038333	12.209433	10.659212
O	13.323841	9.792983	10.558862

9

7B

Np	13.171165	10.979759	11.880673
Np	9.968235	11.688983	10.988593

O	9.794471	12.902089	12.255223
O	14.152724	9.803517	13.034649
O	11.060427	10.418613	12.247340
O	13.135997	12.213633	13.171803
O	9.978786	10.509480	9.678679
O	12.057588	12.220276	10.653944
O	13.325885	9.799459	10.548785

9

7C

Np	12.449306	10.830090	10.838824
Np	12.248901	10.638146	14.272099
O	13.101692	9.319984	9.944633
O	11.400263	11.476897	9.512978
O	11.729583	8.946337	14.293324
O	12.950883	12.228518	14.615499
O	11.259254	11.942705	12.587622
O	10.742933	10.592147	12.495096
O	13.494675	10.365035	12.446455

9

7D

Np	12.360218	10.797114	10.894403
Np	12.316859	10.441625	14.456844
O	13.114591	9.370962	10.012267
O	11.220545	11.113950	9.556285
O	11.823067	8.765003	14.135724
O	12.804268	12.095960	14.868549
O	11.368654	12.226466	12.085764
O	10.857013	10.988954	12.660230
O	13.512278	10.539824	12.336466